PHYSICAL REVIEW LETTERS

Cavitation in a Lubrication Flow between a Moving Sphere and a Boundary

J. Ashmore*

*Department of Applied Mathematics and Theoretical Physics, University of Cambridge,
Wilberforce Road, Cambridge CB3 0WA, United Kingdom*

C. del Pino† and T. Mullin

*Manchester Centre for Nonlinear Dynamics, University of Manchester,
Oxford Road, Manchester M13 9PL, United Kingdom*
(Received 19 October 2004; published 29 March 2005)

A heavy sphere is free to move inside a rotating horizontal cylinder filled with viscous liquid. The steady motion is essentially Stokesian, and the sphere rotates at a fixed location with a lubrication layer between the ball and the wall. The symmetry of the flow field suggests there will be no force to balance the normal component of the ball's weight. However, we show that a normal force can arise when a cavitation bubble is present. The bubble size was measured as a function of the cylinder rotation rate and agrees well with a model which uses the force and torque balances on the sphere.

Introduction.—The motion of a sphere in a Stokes flow along a boundary is a fundamental problem which is relevant to many situations, ranging from bearings [1–3] to the behavior of colloidal suspensions [4]. A heavy sphere moving adjacent to an inclined boundary leads to an interesting long-standing puzzle because the reversibility of Stokes equations and the local symmetry of the flow geometry indicate that no net hydrodynamic force normal to the boundary will arise. Hence, in experiments a heavy sphere is expected to approach the boundary until surface roughness results in contact. However, the measurements of the ratio of the sphere's rotational speed to the wall speed in the experiments we describe here provide evidence of a continuous liquid film separating the sphere and the boundary which provides hydrodynamic lubrication. In this Letter, we show that cavitation breaks the symmetry in the flow and hence a normal force is present, ensuring that the ball does not contact the boundary.

The possibility of cavitation in flows of this type was noted by Taylor [5] and by Goldman *et al.* [6] who found that their theoretical results characterizing the motion of a sphere adjacent to a vertical wall did not agree with available experimental data. They suggested that cavitation is one factor which may account for the discrepancy between theory and experiment, and qualitative results of a model for cavitation were compared with experimental data by Nyrkova *et al.* [7]. Recently, Prokunin [8,9] reported experimental measurements of a sphere moving in a fluid and observed the nucleation of a gas bubble under the sphere.

Cavitation occurs when the component of the sphere's weight tangential to the boundary is sufficiently large that the pressure drops below the vapor pressure, i.e., falls more than 0.1 MPa below atmospheric pressure. The lubrication pressure between the sphere and the wall in our experiments is estimated to deviate from atmospheric pressure by

as much as ±0.3 MPa. For the pressure dependence of viscosity to be significant, the pressure must exceed 10 MPa [10,11]. In cases where the spheres are relatively small or are nearly neutrally buoyant, the pressure will not necessarily fall below the vapor pressure and inertial effects may break the symmetry in the flow [12].

In our experiments a single steel sphere is in the midplane of a horizontal rotating cylinder filled with glycerine. The theoretical model was developed by assuming that the wall is locally planar and that the lubrication layer is unaffected by the outer flow field. Over a range of rotation rates, the ball sits at fixed locations rotating adjacent to the upward moving wall in the bottom quadrant of the cylinder. When the speed of rotation of the cylinder is increased and the ball rises into the upper quadrant, the ball falls from the wall, and the dynamics of this and the low-dimensional chaos observed when multiple balls are present are reported elsewhere [13]. In the present investigation, we study the steady-state attained at lower cylinder rotation rates with the sphere in the lower quadrant, and provide detailed quantitative comparisons between theory and experiment for the motion of the ball and the size of the induced cavitation bubble.

Experimental setup.—The experiment was performed using a horizontal polished glass cylinder with inner radius $L_R = 60.00 \pm 0.02$ mm, wall thickness 4 mm, and length 225 mm. Leveling of the apparatus was maintained to within $\pm 0.1°$ by using a digital inclinometer. The cylinder was filled with degassed glycerine which had a measured shear viscosity of $\mu = 1.12 \pm 0.03$ Pa s at 22.6 °C $\pm$ 0.3 °C and density $\rho_f = 1260 \pm 3$ kg m^{-3}. A dc motor connected via a gear box and a belt drive was used to rotate the cylinder about its axis with velocity U, equivalent to an angular velocity U/L_R. The frequency of the rotation of the cylinder was monitored using an optical shaft encoder

P H Y S I C A L   R E V I E W   L E T T E R S

and was found to be constant to within ± 0.001 Hz. Single smooth chrome steel (EN31) spheres of radius $a = 5, 7.5, 10,$ and 12.5 mm were used in each of the experiments. The tolerance on the diameter, the maximum surface roughness, and the density of the spheres are 2.5 μm, 2 μm, and $\rho_s = 7800 \pm 5$ kg m^{-3}, respectively.

Over a range of rotation rates, the sphere adopted a fixed point and rotated adjacent to the upward moving wall at a fixed angle θ, as indicated in Fig. 1(a). This angle was measured using an engineering protractor. A charge-coupled device camera inclined at an angle θ relative to the horizontal plane was used to monitor the underside of the sphere and thereby enabled estimates of the surface area A_b of the bubble to be made. The bubble diameter in the directions parallel and perpendicular to the direction of motion, denoted by $d_{\parallel}$ and $d_{\perp}$, respectively, and indicated in Fig. 1(b), was measured and the bubble area $A_b = \pi d_{\parallel} d_{\perp}/4$ was calculated. As θ approached 90°, the surface area of the bubble was independently measured using a traveling microscope with accuracy ± 0.01 mm. The angular velocities of the cylinder, U/L_R, and the sphere, ω, were measured using a stopwatch to time the passage of felt pen marks on the surfaces viewed through the traveling microscope. Four measurements were made for each angle θ, and the standard deviation was used to estimate the error.

Model.—We analyze a sphere rotating at rate ω in a semi-infinite fluid bath close to an inclined planar boundary moving at velocity U. When the minimum separation h_0 between the sphere and the boundary is small compared to the sphere radius a, the flow problem is dominated by the narrow gap between the sphere and the boundary. In this region the characteristic length scale parallel to the boundary is $(2h_0 a)^{1/2}$, which is large compared to the characteristic length scale h_0 perpendicular to the plane. Therefore the analysis is based on the lubrication approximation to the Stokes equations. We use a polar coordinate system (r, ϕ) with origin at the point of minimum separation between the sphere and the plane, and with the angle ϕ equal to zero on the line in the opposite direction to the boundary motion.

We denote the deviation from atmospheric pressure by $p(r, \phi)$, the difference between atmospheric and vapor pressure by p_b, and the density difference by $\Delta\rho = \rho_s -$

ρ_f. Nondimensional variables are defined as follows:

$$\mathcal{U} = \frac{\mu U}{\Delta\rho g a^2}, \qquad \Omega = \frac{\omega a}{U}, \qquad \mathcal{H}_0 = \frac{h_0}{a},$$

$$\mathcal{A}_b = \frac{A_b}{2h_0 a}, \qquad \mathcal{P}_b = \frac{p_b}{\Delta\rho g a}, \qquad P = \frac{p}{\Delta\rho g a}, \quad (1)$$

$$R = \frac{r}{(2h_0 a)^{1/2}}.$$

The model uses the force and torque balances on the sphere to calculate $\mathcal{H}_0$, $\mathcal{U}$, and Ω. The bubble area $\mathcal{A}_b$ is determined from conditions related to cavitation. Assuming that the tangential force and torque balances are not significantly affected by the small bubble [8], the results of Goldman *et al.* [6] are valid (see also [14]):

$$\frac{16\pi}{5}\left(1 - \frac{\Omega}{4}\right)\mathcal{U}\ln\left(\frac{1}{\mathcal{H}_0}\right)$$
$$+ 6\pi(0.9588 + 0.2526\,\Omega)\mathcal{U} = \frac{4\pi}{3}\sin\theta, \quad (2)$$

$$\frac{1}{10}(1 - 4\Omega)\ln\left(\frac{1}{\mathcal{H}_0}\right) - 0.1895 - 0.3817\,\Omega = 0, \quad (3)$$

where θ is the angle of inclination of the boundary relative to the horizontal, as indicated in Fig. 1(a). First-order terms in the asymptotic expansion are retained as the expansion in $[\ln(1/\mathcal{H}_0)]^{-1}$ converges relatively slowly.

The force balance normal to the plane is

$$F_N = 2\mathcal{H}_0 \int_0^{2\pi}\int_0^{\sqrt{1/2\mathcal{H}_0}} PR\,dR\,d\phi = \frac{4\pi}{3}\cos\theta, \quad (4)$$

where F_N has been nondimensionalized by $\Delta\rho g a^3$. We approximate the pressure distribution using the lubrication pressure P_{lub} between a rotating sphere and a translating boundary [15], truncated at the vapor pressure to incorporate the effects of cavitation (see Fig. 2): $P(R, \phi) = \max\{P_{\text{lub}}(R, \phi), -\mathcal{P}_b\}$, where

$$P_{\text{lub}}(R, \phi) = \frac{6\sqrt{2}(1 + \Omega)\mathcal{U}}{5\mathcal{H}_0^{3/2}}\frac{R}{(1 + R^2)^2}\cos\phi. \quad (5)$$
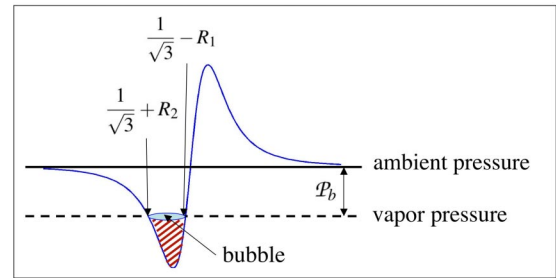
FIG. 2 (color online). Diagram of pressure distribution $P(R, \phi)$ defined by (5) on the axis $\phi = 0$, $\phi = \pi$. The boundary motion is to the left, and the normal force F_N equals the shaded volume.

FIG. 1. (a) Schematic of the experimental setup showing the sphere inside the cylinder. (b) Diagram showing the underside of the sphere, the bubble, and the definition of $d_{\parallel}$ and $d_{\perp}$.

Since the bubble forms in the vicinity of the local minimum of (5) at $R = 1/\sqrt{3}$, $\phi = \pi$, we use $1/\sqrt{3} - R_1$ and $1/\sqrt{3} + R_2$ to denote the bubble's nose and tail on the $\phi = \pi$ axis where the lubrication pressure (5) equals the vapor pressure:

$$P_{\text{lub}}\left(\frac{1}{\sqrt{3}} + R_2, \pi\right) = P_{\text{lub}}\left(\frac{1}{\sqrt{3}} - R_1, \pi\right) = -\mathcal{P}_b. \quad (6)$$

The bubble area is approximated by the area of two semicircles with radii R_1 and R_2:

$$\mathcal{A}_b = \frac{\pi}{2}(R_1^2 + R_2^2). \quad (7)$$

The normal force F_N in (4) equals the volume of the shaded region in Fig. 2 since the lubrication pressure P_{lub} cavitation is antisymmetric, and is approximated by

$$F_N \approx -2\mathcal{H}_0 \int_0^\pi \int_{(1/\sqrt{3})-R_1}^{(1/\sqrt{3})+R_2} \left| R - \frac{1}{\sqrt{3}} \right| P_{\text{lub}}(R, \pi) dR d\phi$$
$$- 2\mathcal{H}_0 \mathcal{P}_b \mathcal{A}_b$$
$$= \frac{12\sqrt{2}(1 + \Omega)\mathcal{U}}{5\mathcal{H}_0^{1/2}}[\mathcal{I}(R_2) + \mathcal{I}(-R_1)] - 2\mathcal{H}_0 \mathcal{P}_b \mathcal{A}_b, \quad (8)$$

where we define

$$\mathcal{I}(R) = \pi \int_{(1/\sqrt{3})}^{(1/\sqrt{3})+R} \left(R - \frac{1}{\sqrt{3}}\right) \frac{R}{(1 + R^2)^2} dR$$
$$= \frac{\pi}{2}\left[\tan^{-1}\left(\frac{1}{\sqrt{3}} + R\right) - \frac{\pi}{6} - \frac{R}{(\frac{4}{3} + \frac{2}{\sqrt{3}}R + R^2)}\right]. \quad (9)$$

Equations (2)–(4) and (6)–(8) are solved using the Newton-Rhapson method to determine $\mathcal{U}$, Ω, $\mathcal{A}_b$, and $\mathcal{H}_0$ for a specified value of the nondimensional vapor pressure $\mathcal{P}_b$.

Experimental measurements and theoretical results.— The cavitation bubble shown in Fig. 3 was observed to be steady and was almost circular: when θ was in the range
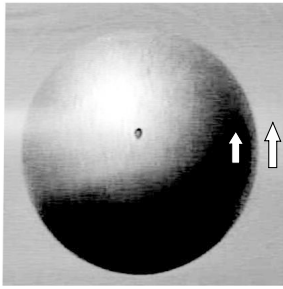
FIG. 3. Photograph of cavitation bubble under 7.5 mm radius sphere at $\theta = 15°$. Both the cylinder wall and the observed surface of the sphere move upwards. The bubble is slightly above the center, as expected.

20° to 70°, the ratio of the diameters $d_\parallel/d_\perp$ was between 1 and 1.2. At extreme angles, the bubble was small and experimental error became significant. When the motion was stopped, the bubble disappeared rapidly, confirming that the bubble was mostly vapor.

The experimental and theoretical results for the bubble area, the boundary velocity, and the sphere's rotational velocity are plotted as a function of angle in Fig. 4, for spheres with different radii. We assume that the liquid cavitates at the vapor pressure since the slight sphere surface roughness provides nucleation sites. The vapor pressure is approximately 0.1 MPa below atmospheric pressure, and therefore the rescaled vapor pressure $\mathcal{P}_b$ in the model is calculated using $p_b = 0.1$ MPa. In general,
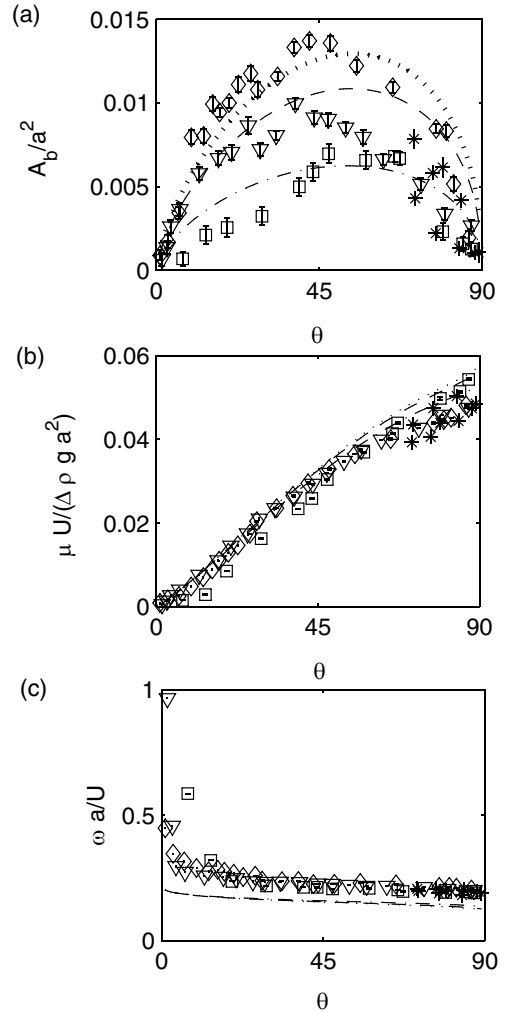
FIG. 4. Experimental and theoretical results for (a) rescaled bubble surface area A_b/a^2, (b) the nondimensional boundary velocity, and (c) the sphere's rotational velocity. Points (experiments) and lines (theory) for spheres of radii 5 mm (squares, dash-dotted line), 10 mm (triangles, dashed line), and 12.5 mm (diamonds, dotted line). Data denoted by asterisks in (a) were measured using a traveling microscope. Error bars are indicated but are smaller than the symbols in (b) and (c).
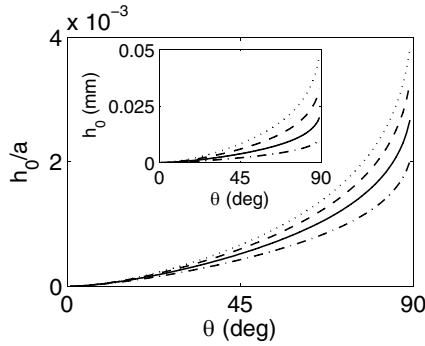
FIG. 5. Theoretical results for the nondimensional and (inset) dimensional minimum separation between the sphere and the boundary, for spheres with radii 5 mm (dash-dotted line), 7.5 mm (solid line), 10 mm (dashed line), and 12.5 mm (dotted line).

the experimental and theoretical results agree well; the larger values of $\omega a/U$ at very small angles may indicate where roughness becomes significant [4].

It proved very difficult to obtain reliable experimental estimates of the minimum separation h_0 between the sphere and the boundary. The value predicted using Eqs. (2)–(4) and (6)–(8) is plotted in Fig. 5 and is on the order of 10 μm, which exceeds the roughness scale of 2 μm. Therefore roughness effects are negligible, except perhaps at small angles. The theoretical value of h_0 is used to estimate the maximum pressure, which is of order 0.3 MPa, and the lubrication Reynolds number $\rho U h_0^{3/2}/(\mu a^{1/2})$, which is approximately 2.5×10^{-4}. These values suggest that neglecting the pressure dependence of viscosity, elastohydrodynamic boundary deformation and inertia is justified. The capillary pressure is negligible since the surface tension divided by the separation gives an estimated value of 7 kPa, which is small compared to $p_b = 100$ kPa. Finally, approximating the cylindrical boundary of the experiment by a plane in the model corresponds to a geometric rescaling. We do not expect the approximation involved to introduce a significant error in the estimates of the force and torque balances. A detailed calculation is planned to check this.

Conclusions.—We have demonstrated that, in a lubrication geometry in low Reynolds number flow, cavitation can occur. In the context of a sphere moving close to a plane, arguments based on the symmetry of the flow break down when a cavitation bubble is present, and the flow can exert a force on the sphere which balances the normal component of the sphere's weight, preventing the sphere and boundary from making contact.

The rescaled bubble area and minimum separation between the sphere and the boundary both increase as the nondimensional vapor pressure $p_b/(\Delta \rho g a)$ decreases, whereas the rescaled boundary velocity and the sphere's rotation rate do not vary significantly with this parameter. An intuitive explanation for these results is that the tangential force and torque balances, which primarily determine U and Ω, are not strongly affected by the bubble or by the value of the minimum separation between the sphere and the boundary, whereas the normal force balance which determines the separation between the sphere and the boundary is affected by the bubble. The theory predicts that the minimum separation is on the order of 10 μm in these experiments, and increases as a function of angle and as the sphere radius increases. We expect these results are also relevant to nonspherical convex objects, such as spheroids moving close to a boundary.

*Electronic address: J.Ashmore@damtp.cam.ac.uk
†Permanent address: ETSII, Universidad de Malaga, Spain. Electronic address: cpino@uma.es.

[1] D. Dowson and C. M. Taylor, Annu. Rev. Fluid Mech. **11**, 35 (1979).
[2] B. J. Hamrock, *Fundamentals of Fluid Film Lubrication* (McGraw-Hill, New York, 1994).
[3] A. Z. Szeri, *Fluid Film Lubrication: Theory and Design* (Cambridge University Press, Cambridge, 1998).
[4] Y. Zhao, K. P. Galvin, and R. H. Davis, Int. J. Multiphase Flow **28**, 1787 (2002).
[5] G. I. Taylor, J. Fluid Mech. **16**, 595 (1963).
[6] A. J. Goldman, R. G. Cox, and H. Brenner, Chem. Eng. Sci. **22**, 637 (1967).
[7] I. A. Nyrkova *et al.*, J. Phys. II (France) **7**, 1709 (1997).
[8] A. N. Prokunin, Fluid Dyn. **38**, 443 (2003).
[9] A. N. Prokunin, Fluid Dyn. **39**, 771 (2004).
[10] R. L. Cook *et al.*, J. Chem. Phys. **100**, 5178 (1994).
[11] P. L. Kapitza, *Collected Papers of P. L. Kapitza, Vol. II (1938–1964)* (Pergamon, Oxford, 1965).
[12] M. R. King and D. T. Leighton, Phys. Fluids **9**, 1248 (1997).
[13] T. Mullin *et al.*, J. Appl. Math. (to be published).
[14] G. S. Perkins and R. B. Jones, Physica (Amsterdam) **189A**, 447 (1992).
[15] M. E. O'Neill and K. Stewartson, J. Fluid Mech. **27**, 705 (1967).